APPLIED AND ENVIRONMENTAL MICROBIOLOGY, Dec. 1984, p. 1151–1158
0099-2240/84/121151-08$02.00/0

Vol. 48, No. 6

Multiplicity of Aspartate Transport in Thin Wastewater Biofilms

T. TAYLOR EIGHMY* AND P. L. BISHOP

Department of Civil Engineering, University of New Hampshire, Durham, New Hampshire 03824

Received 17 April 1984/Accepted 20 August 1984

This research documents the multiplicity of L-aspartate transport in thin wastewater biofilms. A Lineweaver-Burk analysis of incorporation produced a curvilinear plot (concave down) that suggested active transport by two distinct systems (1 and 2). The inactivation of system 2 with AsO_4 or osmotic shock resolved system 1, which was a high-affinity, low-capacity system with an apparent K_t (Michaelis-Menten constant) of 4.3 μM (AsO_4) or 4.6 μM (osmotic shock). The inactivation of system 1 with dinitrophenol resolved system 2, which was a low-affinity, high-capacity system with an apparent K_t of 116.7 μM. System 1 was more specific for aspartate than system 2 in the presence of aspartate analogs. Sodium had no discernible effect on the incorporation velocities by either system. These results indicate that system 1 is a membrane-bound proton symport coupled to the proton gradient component of the proton motive force and that system 2 is a binding protein-mediated system coupled to phosphate bond energy. Analyses of diffusional limitations on the derived transport constants indicated that internal resistances were present but that the apparent constants were close to the intrinsic values, especially for system 1. Metabolic inactivation of the biofilm with dinitrophenol and AsO_4 did not completely inactivate aspartate incorporation, which indicated that some simple adsorption of the aspartate anion by the biofilm had occurred. These results show that aspartate is transported by wastewater biofilm bacteria via systems with different affinities, specificities, and mechanisms of energy coupling.

Biofilms are used in a number of fixed-film wastewater treatment schemes, including rotating biological contactor, fixed-bed, and fluidized-bed processes. Biofilms provide treatment by removing soluble and hydrolyzable colloidal substrates from the waste stream. The substrates in the waste stream are a diverse mixture of soluble fatty acids and sugars, colloidal proteins and carbohydrates (41, 42), and soluble amino acids (8, 52); the relative percentages of these substrates vary over time. Substrate removal is a complex combination of mass transfer and metabolic processes. One of the important events in this sequence is the active transport of the substrate from the region near the cell, across the cell membrane, and into the cytoplasm. Despite its importance to wastewater treatment, there has been no research to date on the specific properties of substrate transport systems in biolfilm bacteria, although La Motta (37) reports that laboratory-grown biofilms exhibit saturation kinetics for glucose uptake.

There are a number of carrier-mediated substrate transport systems present in bacteria, and the mechanisms for coupling chemical energy to translocation are varied (13, 47). The coupling processes for two of these systems were elucidated by Berger (9) and by Berger and Heppel (10) with *Escherichia coli*. They showed that an electrochemical proton gradient generated by a proton motive force (PMF) is sufficient to drive membrane-bound transport systems, whereas phosphate bond energy is necessary to drive another, separate system which requires a water-soluble, periplasmic binding protein for transport.

Aspartate transport is one of the better-documented active transport processes in bacteria (5). Aspartate is generally transported by two distinct systems. One involves the membrane-bound proton symport (17, 40), which is coupled to the proton gradient of the PMF and actively transports the aspartate molecule in conjunction with a proton. It is present in membrane vesicle preparations of gram-negative (27, 38, 55) and gram-positive (33, 34, 50, 54) bacteria. This system also remains functional in osmotically shocked cells but is inactivated by uncouplers such as dinitrophenol (DNP). The other involves the periplasmic binding protein found in gram-negative bacteria (1, 55, 56), which requires phosphate bond energy (13) for active transport. It is inactivated by the phosphate analog arsenate (AsO_4), and it is removed from gram-negative cells by osmotic shock (1, 13, 55) and by the processes of spheroplast and vesicle formation. There are, however, exceptions to these transport schemes (23, 49, 56, 60). Furthermore, complex incorporation kinetics are observed when a Lineweaver-Burk analysis of aspartate incorporation in whole cells produces a curvilinear, or biphasic, plot that is concave down (44, 56). This complexity is attributed to heterogeneous aspartate transport by the two systems present in the bacterium that correspond to the two systems described above (28, 49) and in a few cases to negative cooperation (18) or possibly to allosteric effects (21, 22) in one homogeneous membrane-bound system. Resistance to diffusional mass transfer can also affect the linearity of the transformed data (15, 24, 59), especially if the transformations used are sensitive to the effects of such resistance.

Our research was conducted to see whether multiplicity of aspartate transport was present in thin wastewater biofilms established in situ and composed largely of gram-negative bacteria (14). Aspartate was selected as the substrate because it is present in waste water (52) and its transport systems are well documented. Kinetic analyses of aspartate incorporation by adhering biofilms subjected to a number of treatments were used to resolve individual transport systems. We report here the presence of two separate and distinct aspartate transport systems in the thin wastewater biofilms that we examined.

(Portions of this material were presented at the Second International Conference on Fixed-Film Biological Processes, Washington, D.C., 10 to 12 July 1984.)

* Corresponding author.

MATERIALS AND METHODS

Biofilm sampling device. We used tubular sampling devices suitable for submersion in a waste stream and subsequent bacterial colonization. A sampling device is shown in Fig. 1. The details of their construction are given elsewhere (14).

Thin biofilms (less than 60 μm thick after rinsing) were used in the transport assays to minimize diffusional resistances within the biofilm (36, 37). The biofilms were allowed to develop for no more than 18 days on the basis of previous work (14). The biofilms were formed by placing clean sampling devices in a weighted rack and submerging it in a flowing channel at the Durham, N.H., Wastewater Treatment Facility. The waste stream contained domestic primary effluent and recycled activated sludge microorganisms. The rack was oriented in the channel so that waste water could flow through the tubes at very low velocities. Sampling tubes with biofilms of known age were returned to the lab and maintained in dilute (10%) primary effluent before use. In all instances, loosely bound bacteria were removed from the sampling stub by gentle rinsing, so that firmly adhered bacteria were present on the stub.

Scanning electron microscopy. Samples were prepared for scanning electron microscopy by the methods outlined by Eighmy et al. (14). Sampling stubs (Fig. 1) were separated from the nylon screw with a razor and fixed in 5% glutaraldehyde for 1 h at 20°C. Samples were dehydrated in a graded ethanol series before critical-point drying in a Samdri Critpoint dryer. The stubs were sputter coated with a 60:40 gold-palladium mixture in a Technics Hummer V sputter coater. The biofilms were examined with an AMR 1000 scanning electron microscope at a 20-kV accelerating potential. The biofilms were then photographed with the specimen stage tilted to 11°. Numerous stubs were viewed to ensure representative sampling.

Osmotic shock treatment. Osmotically shocked biofilm samples were prepared by the method of Anraku and Heppel (6). Groups of four sampling stubs were exposed to 10 ml of a pretreatment solution containing 3.3×10^{-2} M Tris (pH 7.3), 1×10^{-4} M EDTA, and 20% (wt/vol) sucrose for 10 min at room temperature. The stubs were rinsed with a cold (4°C) shock solution containing 5×10^{-4} M $MgCl_2$ and then held in that solution at 4°C for 10 min. The stubs were then transferred to 20°C buffered tap water (BT) before they were used in transport assays. The BT solution (pH 6.8) contained 5 mM KH_2PO_4 and 5 mM K_2HPO_4.

Inactivation treatments. Resolution of the individual transport systems was also accomplished through the selective use of a poison or uncoupler. For the uncoupler DNP, samples were treated by preincubation for 1 min before and then during the assay in 2.0 mM DNP in BT (60). The duration of preincubation with DNP was important for resolving the DNP-insensitive system. Preliminary work indicated that both 10- and 5-min preincubations in 2.0 mM DNP disrupted all aspartate transport, but that the PMF-dependent aspartate transport system was not inactivated without incubation. A 1-min preincubation proved satisfactory for producing a Lineweaver-Burk plot with good linearity. For the phosphate analog AsO_4, samples were treated by preincubation for 15 min before and then during the assay in 10 mM AsO_4 in BT (51).

Influence of sodium on transport. The effect of Na^+ on aspartate incorporation was determined by including 10 mM NaCl in the incubation solution during the transport assays (39).

Transport assays. A modification of the procedure employed by Vaccaro and Jannasch (53) was used to determine incorporation velocities. Concentrated soluble L-aspartate was used to vary the substrate concentrations, and a low level of L-[U-^{14}C]aspartate (approximately 3.0×10^{-2} μCi · ml^{-1}) was used as the tracer. The velocities of incorporation were determined with the following expression: $V = (fS)(tA)^{-1}$, where V is the initial incorporation velocity (in nanomoles per hour per square centimeter of biofilm), f is a fraction relating the disintegrations per minute incorporated into the biofilm to the total initial disintegrations per minute in the entire incubation solution, S is the initial total substrate mass in the incubation solution (in nanomoles), t is the

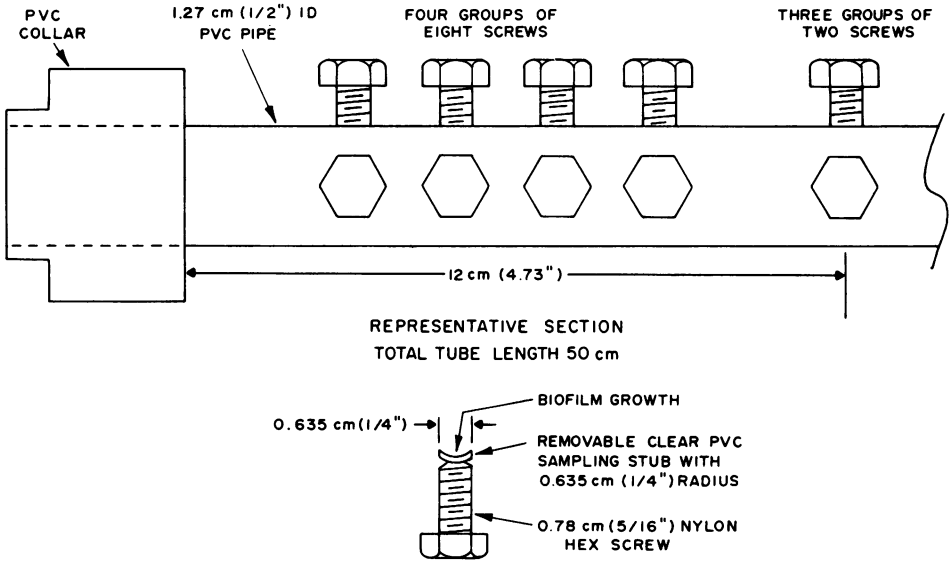

FIG. 1. Schematic of the tubular sampling device. It consists of the support structure (polyvinyl chloride [PVC] pipe with 38 threaded holes, above) and 38 sampling stubs with screws (one is shown below). Screws with clean stubs are threaded into the pipe so that the pipe interior is hydraulically smooth. The adsorption and growth of bacteria take place on the stub surface.

incubation period (in hours), and A is the area of a sampling stub (in square centimeters). Velocities were corrected for biofilm mass by dividing by the appropriate total organic carbon (TOC) value (in milligrams of TOC per square centimeter of biofilm) so that the actual units for velocity of incorporation were nanomoles per hour per milligram of TOC.

All assays were done in a dark incubator at 20°C in Whirl-Pak bags. The incubation solutions contained BT and label. Six samples (0.5 ml each) of this solution were taken before the assay to determine the counts per minute in the solution for use in the equation. Appropriate concentrations of unlabeled aspartate (0.5 ml) and, for inhibition or sodium assays, of DNP (0.5 ml), AsO_4 (1.0 ml), or NaCl (0.5 ml) were then added to the bag so that the final volume was 10 ml. Assays were begun by adding four stubs to a bag. Previous work (27, 28, 33, 34, 44, 45, 50, 54, 56) indicates that a 5-min incubation is adequate to produce linear uptake with an intercept through the origin, and therefore 5-min incubations were used. This kept the change in the aspartate concentration in the incubation solution to less than 1%. The incubations were terminated by adding 1 ml of 1% buffered Formalin (pH 7.3) for a 5-s contact time (19). The bags were drained, and the stubs were rinsed three times with BT. Preliminary studies indicated that the Formalin treatment did not result in a loss of incorporated label from the biofilm and that the BT rinse was sufficient to remove any respired label, if present, from the biofilm. The biofilms were solubilized by adding a stub to a 7-ml Solvent Saver scintillation vial (Kimball Co.) containing 0.5 ml of a 1:1 Protosol (New England Nuclear Corp.)-ethanol mixture. All liquid scintillation counting was done in approximately 4.5 ml of Dynagel cocktail (J. T. Baker Chemical Co.), and 50 μl of glacial acetic acid was added to minimize chemiluminescence. Radioactivity was measured with a Beckman 700 liquid scintillation counter. Counts per minute were converted to disintegrations per minute by correcting for background, machine efficiency, and counting efficiency. Where applicable, the apparent transport constants K_t (Michaelis-Menten constant) and V_{max} (maximum velocity of the system) were derived from Lineweaver-Burk transformations of the data by using a least-squares regression analysis to produce a line of best fit. Eadie-Hofstee and Hanes transformations were performed as well for comparative purposes.

Analysis of diffusion effects on transport kinetics. To evaluate the influence of diffusional resistances on the transport kinetics of the aspartate transport systems in the biofilm bacteria, we used the graphing procedure of Engasser and Horvath (15, 24). The method uses dimensionless parameters in an Eadie-Hofstee-type plot in which the shape of the curve is indicative of the type and degree of diffusional resistance (external or internal) present in the transport assay. To use the procedure, it was necessary to visually estimate the transport constants (K_t and V_{max}) from plots of uptake versus substrate concentration.

TOC determinations. The TOC content of the adhering biofilms was assayed by the following procedure. Twenty stubs with biofilms of known age were stored in a desiccator until analysed. The ampoule method outlined for the Oceanography International model 526 TOC analyzer (Oceanography International Corp., College Station, Tex.) was used. One stub was digested per ampoule. The biofilm TOC values were corrected for the stubs by running clean stubs as controls. Glucose was used as a standard.

Analog specificity studies. The specificity of the transport systems were assayed by determining the percent inhibition of labeled aspartate incorporation in the presence of 10^{-3} M of an analog (1, 12, 28). The appropriate poison or inhibitor was used as described above. The concentration of the label in the Whirl-Pak bag was 0.1 $\mu Ci \cdot ml^{-1}$.

Adsorption studies. The potential for adsorption of aspartate by the biofilm was determined as follows. Biofilms were inactivated simultaneously by DNP (5-min preincubation) and AsO_4 as described above before being incubated with labeled aspartate (0.1 $\mu Ci \cdot ml^{-1}$) for 5 min. Untreated controls were run for comparison.

Chemicals. L-[U-^{14}C]aspartate (specific activity, >200 $mCi \cdot mmol^{-1}$) and Protosol were obtained from New England Nuclear Corp., Boston, Mass. All other chemicals and analogs were obtained from Sigma Chemical Co., St. Louis, Mo., and were the highest possible reagent grade.

RESULTS

Biofilm characteristics–scanning electron microscopy. A diverse group of microorganisms was found firmly adhering to the stub surfaces (Fig. 2A). Both filaments and rods were present. At least four distinct morphologies were observed. The distribution of the organisms on the biofilm was patchy and clumped, although some samples were composed of a continuous film of rods and filaments enmeshed in a slime material (Fig. 2B). This material corresponded to the type 1 glycocalyx which we observed in another study (14). Estimated biofilm thicknesses ranged from 20 to 60 μm; these estimates were determined by comparing the biofilms with other biofilms of similar composition and known thickness (14).

Biofilm TOC. The near-linear increase in biofilm TOC over time was attributed to the colonization and growth of firmly adherent microorganisms (Fig. 3). The mean TOC values shown in Fig. 3 were used to determine the velocity of incorporation by biofilms of corresponding ages.

Aspartate incorporation. The Lineweaver-Burk plot of aspartate incorporation velocities by untreated biofilms was curvilinear and concave down (Fig. 4). Its similarity to curvilinear plots shown elsewhere suggested a heterogeneous transport process by two systems (28, 60). Both Eadie-Hofstee and Hanes transformations of the data also resulted in curvilinear plots with good correlation.

Resolution of systems 1 and 2. System 1 was resolved by inactivating system 2 with either AsO_4 or osmotic shock treatment (Fig. 5). Both treatments produced nearly identical apparent K_t and V_{max} values based on Lineweaver-Burk transformations of the data (Table 1). The other transformations produced similar apparent kinetic constants. System 1 was classified as a high-affinity, low-capacity system. System 2 was resolved by DNP treatment of system 1 (Fig. 6). The apparent K_t and V_{max} values for system 2 derived by a Lineweaver-Burk transformation of the data differed from those of system 1 (Fig. 6). System 2 was classified as a low-affinity, high-capacity system. The other two transformations, which supported the classification of system 2 as a low-affinity, high-capacity system, were not in as good agreement with the Lineweaver-Burk-derived constants. We chose to base our interpretation of the data for both systems on the Lineweaver-Burk-derived kinetic constants because of the wide use of that method in the literature.

We also observed, via the regression-derived velocities for system 1 (Fig. 5, AsO_4 inactivation) and system 2 (Fig. 6), that the sum of the velocities for systems 1 and 2 was greater when the systems operated individually than when they operated simultaneously. This suggested to us that the potential velocity of incorporation for the two systems was

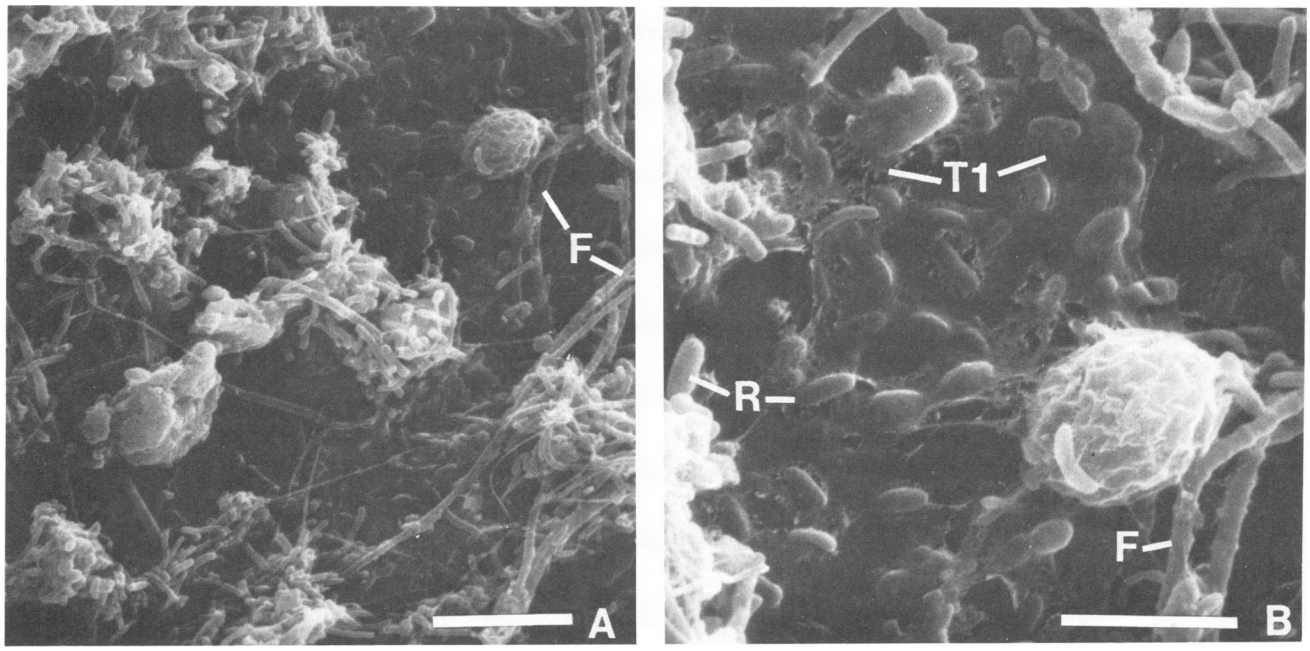

FIG. 2. Representative scanning electron micrographs of the firmly adherent biofilm community. The biofilm is 16 days old. Symbols: F, filament; R, rod; T1, type 1 glycocalyx. (A) Note the diverse morphologies and biofilm clumping (bar, 10 μm). (B) Detail of panel A. Note the slime material (type 1 glycocalyx) around the cells and on the stub surface (bar, 5 μm).

not attained when the two systems were operating simultaneously and competing for substrate.

Influence of sodium on systems 1 and 2. The presence of 10 mM NaCl in the incubation medium had no discernible effect on either system, as an incorporation curve and its Lineweaver-Burk plot were similar to those of a control (data not shown) in their curvilinear shape and magnitude (see Fig. 4).

Specificities of systems 1 and 2. The specificity of each system for L-[*U*-^{14}C]aspartate is shown in Table 2. System 1 was specific, as unlabeled L-aspartate produced the highest percent competition. The presence of an α-amino group was important for substrate recognition in this system, because four carbon dicarboxylic acids were not effective competitors. System 1 preferred the L-isomer over the D-isomer. It also tolerated substitutions on the β-carbon, because these substances were the most effective competitors. Substitutions on the amino nitrogen were tolerated as well. Analogs with substitutions on the α-carbon were not as effective in competing with labeled aspartate for the transport protein. The chain length of the dicarboxylic amino acid was not as important for recognition as long as the α-amino group was present, because glutamate was somewhat competitive in this system. Higher-molecular-weight analogs which had α-amino groups were also effective competitors. The generally high percentages of inhibition reported here were due to the high concentration of analog in the incubation solution (28).

System 2 was less specific than system 1 as a variety of analogs were more competitive than unlabeled L-aspartate in recognizing the transport system. System 2 was less stereospecific, and substitutions on both α- and β-carbons were

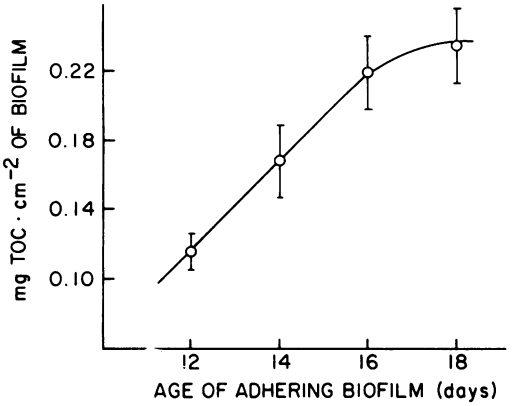

FIG. 3. Mean adherent biofilm TOC values as a function of the time of biofilm development. The means are averages of 20 individual values, and the standard deviation is shown as a vertical line.

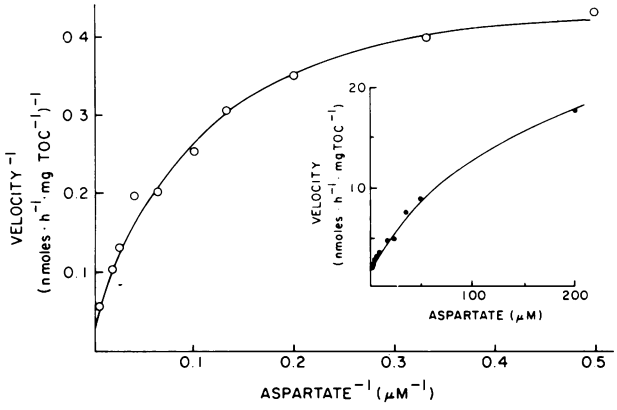

FIG. 4. Lineweaver-Burk plot of aspartate incorporation by untreated biofilms. The mean values are averages of individual incorporation velocities for eight stubs at each substrate concentration. The average percent standard deviation about the means was 16.0%. (Inset) Plot of velocity versus substrate concentration for the data represented in the Lineweaver-Burk plot.

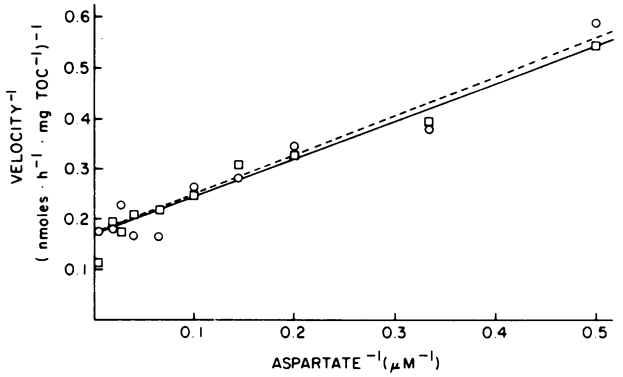

FIG 5. Lineweaver-Burk plots of aspartate incorporation by system 1 as revealed by AsO_4 (□—□) or osmotic shock treatment (○----○) of system 2. The mean values (○, □) are averages of individual incorporation velocities for eight stubs at each substrate concentration. The average percent standard deviations about the means were 26.0% for AsO_4 and 18.8% for osmotic shock values. The least-squares regression for each set of data produced lines of best fit (—, ---) for the data. See Table 1 for K_t, V_{max}, and r.

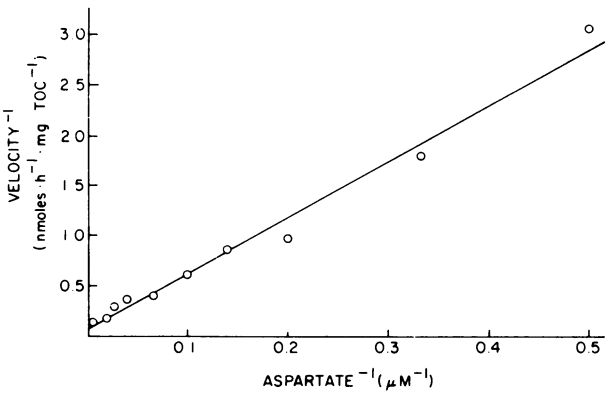

FIG. 6. Lineweaver-Burk plot of aspartate incorporation by system 2 as revealed by DNP treatment of system 1. The mean values are averages of individual incorporation velocities for eight stubs at each substrate concentration. The average percent standard deviation about the means was 16.4%. The least-squares regression for the data produced the line of best fit for the data. See Table 1 for K_t, V_{max}, and r.

tolerated. The presence of an α-amino group was not as important in substrate recognition, because dicarboxylic acids were effective competitors.

Analysis of diffusional effects. By using the Engasser and Horvath graphing method of analysis (15, 24) on the derived data when both systems were functional, a concave-up curve could be fitted to the data points. The shape of the curve suggested that strong internal diffusional resistance had occurred during the assays. When the procedure was employed for the derived data for system 1 or 2 alone, however, a slightly sigmoidal curve could be fit to the data points for either system. The shape of these curves suggested that small internal diffusional resistances were present during the assays. Because the mass transfer conditions were identical in all the assays, it is probable that the strong resistance indicated by the data that were derived when both systems were functional was more a result of the biphasic nature of the curve.

TABLE 1. Apparent kinetic constants of the aspartate transport systems in the wastewater biofilm[a]

System resolved (method)	Transformation method[b]	K_t (μM)	V_{max} (nmol · h^{-1} · mg of TOC^{-1})	r[c]
1 (AsO_4)	LB	4.3	5.9	0.97
	EH	5.1	6.4	vg
	H	14.1	8.7	0.99
1 (osmotic shock)	LB	4.6	5.9	0.97
	EH	4.1	5.9	g
	H	3.9	6.7	0.99
2 (DNP)	LB	116.7	20.3	0.99
	EH	44.8	9.0	g
	H	60.0	10.9	0.98

[a] Based on linear regressions or subjective line of best fit of mean incorporation velocities from data shown in Fig. 5 and 6.
[b] Methods of linearization of data were Lineweaver-Burk (LB), Eadie-Hofstee (EH), and Hanes (H) transformation.
[c] Correlation coefficient for linear regressed data. With the Eadie-Hofstee plot, the goodness of fit is subjectively described as very good (vg) or good (g).

Adsorption studies. In the absence of inhibitors, the mean (± percent standard deviation; n = 10) radioactivity was 1,892 dpm ±31%, compared with 166 dpm ±28% after simultaneous inhibition with AsO_4 and DNP. The percent incorporation without inhibitors was 100%. When the aspartate transport systems in the biofilm were simultaneously inhibited by AsO_4 and DNP, there was still a small percentage (8.8%) of incorporation, which suggested that some simple adsorption of aspartate by the biofilm had occurred.

DISCUSSION

This study shows that two L-aspartate transport systems were present in thin wastewater biofilms composed of firmly adhering rods and filaments. Previous work shows that these bacteria are predominantly gram-negative (14). This work is

TABLE 2. Specificity of systems 1 and 2 for [^{14}C]aspartate uptake in the presence of an analog[a]

Analog[b]	% Competition[c]	
	System 1	System 2
None (inhibitor only)	0	0
L-Aspartate	98.0	87.1
Citrate	1.0	70.9
Succinate	54.0	46.9
Fumarate	3.7	68.5
L-Malate	37.2	76.1
L-Cysteate	42.7	89.0
L-Glutamate	70.9	74.7
D-Aspartate	59.8	92.4
N-Formyl-L-aspartate	85.0	90.5
N-Methyl-L-aspartate	61.9	65.1
α-Methyl-DL-aspartate	81.8	61.3
β-Methyl-DL-aspartate	57.4	91.4
L-Aspartate dibenzyl ester	78.5	76.6
β-Benzyl-L-aspartate	93.4	80.0
L-Aspartate di-*t*-butyl ester	36.0	23.5
L-Aspartate-β-hydroxamate	92.0	93.3

[a] Concentration of L-[*U*-^{14}C]aspartate was 0.1 μCi · ml^{-1} (4.6×10^{-4} μM).
[b] Analog concentration was 10^{-3} M.
[c] Based on means from four stubs for each analog and system. The average percent standard deviations for the means were 29% for system 1 and 21% for system 2. System 2 was inactivated with AsO_4 to study system 1. System 1 was inactivated with DNP to study system 2.

significant in demonstrating that substrates can be translocated by wastewater biofilm bacteria via transport systems with different affinities, specificities, and mechanisms of energy coupling.

Aspartate incorporation by untreated biofilms resulted in a curvilinear, or biphasic, Lineweaver-Burk plot. Curvilinear aspartate incorporation plots have been reported for a number of bacterial species. In gram-negative bacteria, this curvilinearity is attributed to heterogeneous transport systems (28, 49, 56). In gram-positive bacteria, curvilinearity (44, 45, 54) is usually attributed to negative cooperation (18), although allosteric effects have been suggested (21, 22). To determine whether negative cooperation adequately explained our data, we analyzed the data presented in Fig. 4 with a Hill plot, using the method described by Glover et al. (18), and obtained a slope of 0.80. Although this value indicates a slight negative cooperation,, we feel that the resolution of two separate and distinct aspartate transport systems is evidence of heterogeneity. Heterogeneous transport for a number of dicarboxylic acids (29, 30) and amino acids (2, 16, 20, 25, 31, 43, 48, 57, 60) has been reported for a variety of gram-negative bacteria.

System 1 was classified as a high-affinity, low-capacity, membrane-bound proton symport for the following reasons. (i) Its apparent K_t was very similar to those reported for aspartate transport by membrane-bound symports in other gram-negative bacteria (1, 27, 28, 38, 49), although it exhibited a greater affinity than the membrane-bound symports reported for gram-positive bacteria (33, 34, 44, 45, 40, 54). (ii) System 1 was insensitive to treatments (AsO_4 and osmotic shock) that are used to inactivate binding protein-mediated systems while leaving intact membrane-bound PMF-dependent systems (13, 32, 60). (iii) System 1 was sensitive to a treatment (uncoupling) which is used to inactivate the PMF-dependent system (13, 32, 60). (iv) System 1 also exhibited a degree of specificity for aspartate that is usually associated with a membrane-bound system (1, 28). (v) Glutamate is translocated by membrane-bound porters in conjunction with a sodium ion (5, 27, 39), which has led some to speculate that aspartate may be a sodium cotransport system as well (49). We did not detect any enhanced substrate transport in the presence of sodium, which agrees with the data of Kahane et al. (27) and the opinion of Anraku (5) and indicates that the membrane-bound system in the wastewater biofilm was a proton symport at the pH (6.8) of the incubation medium.

System 2 was classified as a low-affinity, high-capacity, binding protein-mediated system for the following reasons. (i) It was inactiviated by the phosphate analog AsO_4, which is used to inactivate binding protein systems that are directly coupled to phosphate bond energy (51). (ii) System 2 was inactivated by osmotic shock treatment, which is also used to inactivate binding protein systems (13). (iii) System 2 was also insensitive to uncoupling, although the duration of incubation with DNP was important in its resolution. (iv) System 2 exhibited a specificity for aspartate that is associated with a binding protein-mediated system (1). The apparent affinity (K_t) of system 2 for aspartate, however, was two orders of magnitude less than the dissociation constants (K_d) for aspartate-binding proteins in vitro (1, 55, 56). Usually K_t and K_d are quite similar (58), and therefore there is a discrepancy between the reported values and the one determined for system 2.

There are problems with using uncouplers such as DNP to inactivate a PMF-dependent system to resolve a binding protein-mediated system (48, 60). Uncouplers accelerate the depletion of ATP pools because the BF_0F_1 ATPase complex (the membrane-bound enzyme with its F_0 and F_1 subunits) attempts to establish a proton gradient, and consequently less phosphate bond energy (ATP) is available to drive the binding protein-mediated system. The DNP treatment we employed did yield a linear plot that fit the lower portion of the incorporation curve shown in Fig. 4. The sensitivity of system 2 to uncouplers indicates that some error may be associated with the V_{max} determined for system 2; however, its apparent K_t should have remained unaffected. Bright and Fletcher (11) indicate that the V_{max} for specific amino acid transport systems associated with an adhering *Pseudomonas* sp. may also be a function of the surface properties of the substratum to which the bacterium adheres.

The kinetic constants which we derived for both systems are the apparent rather than the intrinsic constants (15, 24, 36, 59). Analyses of the effects of diffusional limitations on the derived constants indicate, however, that slight internal resistances within the biofilm matrix were present but that the apparent constants are probably close to the intrinsic values, especially for system 1, the K_t of which was similar to those reported for cells assayed while in suspension, where resistances are minimal. The fact that the K_t values were close to intrinsic was probably the result of the short incubation time of the transport assays which did not allow a substrate concentration gradient to develop.

The interpretation of the data presented here is difficult because a mixed bacterial population constituted the biofilm. Multiphasic transport kinetics for glucose (7) and cyclic AMP (3) have been observed in marine microbial assemblages. Ammerman and Azam (3) attribute the separate kinetic phases for cyclic AMP transport to overlap among the individual systems of the species present in the assemblage. The two systems we observed may have belonged to two separate bacterial species, or they both may have been common to one or more of the species present in the biofilm. The latter possibility is not unreasonable, because heterogeneous transport in a gram-negative bacterium is common and these biofilm bacteria are gram negative (14).

A bacterium that has both systems has ecological advantages. System 1 was the predominant transport mechanism at low external substrate concentrations, whereas system 2 predominated when the substrate levels were high (Fig. 7). Kay (28) suggests that the high-affinity aspartate transport system in *Escherichia coli* specifically transports aspartate as a source of nitrogen, whereas the low-affinity system transports aspartate as a carbon source for growth because of its greater transport capacity. Additionally, the bacterium can use both systems under anaerobic conditions in the absence of a suitable electron acceptor as long as substrate-level phosphorylation occurs to make ATP (or phosphate bond energy) available (i) for the BF_0F_1 ATPase complex to pump out protons and establish a proton gradient or (ii) to directly couple the binding protein system. The potential for competition between the two systems exists when the aspartate concentration is between 40 and 80 μM and the percent contributions to total uptake are similar (Fig. 7). Competition between the two systems was also indicated when their potential velocities were not attained during simultaneous operation. The concept of competition between the two systems is not unreasonable considering that the sites for transport by either system are probably situated adjacent to one another in the cytoplasmic membrane of at least one of the morphological types present in the biofilm.

When both systems were inactivated with DNP and AsO_4, a small percentage (compared to controls) of aspartate was

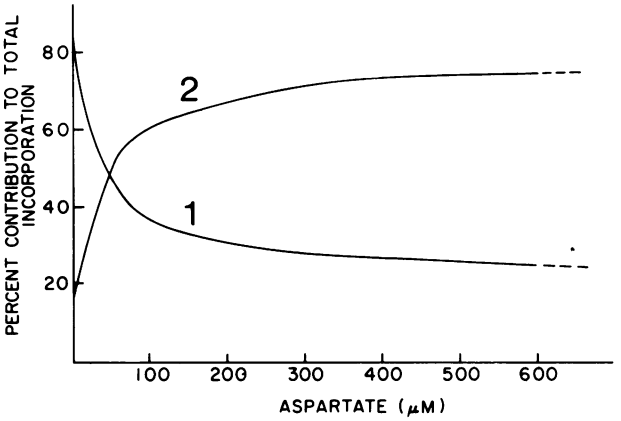

FIG. 7. Percent contribution by each system to total incorporation. The lines of best fit for system 1 (AsO_4 treatment) and system 2 (DNP treatment) were used to determine velocities over a range of substrate concentrations. The predicted velocities of each system were summed and percentages were calculated and depicted graphically

taken up by the biofilm. If we assume that the treatments were sufficient to inactivate both systems completely, then the data suggest that some type of adsorption had occurred. The biofilm was enmeshed in a spatially extensive extracellular slime (Fig. 2). This material, which corresponds to the type 1 glycocalyx, is densely polyanionic (14). At the pH of the incubation solution (6.8), aspartate has a net negative charge, and specific adsorption could occur if the free energy of adsorption were negative. Adsorption of inorganic anions (46) and amino acid dipolar ions (26) by microbial extracellular material has been documented.

In conclusion, the results presented here indicate that aspartate incorporation by biofilm bacteria is mediated by separate transport systems with different affinities, specificities, and mechanisms of energy coupling. Such heterogeneous transport systems are usually subject to environmental and genetic control (4, 31, 35). The heterogeneity reported here may be typical for other soluble substrate transport systems in wastewater biofilm bacteria, which indicates that substrate removal in fixed-film wastewater treatment processes is more complex than has been assumed.

ACKNOWLEDGMENTS

We thank Eva Kashket, William Chesbro, and Nancy Kinner for helpful discussions of this work.

We also thank Paul Ossenbruggen and the Department of Civil Engineering for financial support of certain aspects of this research.

LITERATURE CITED

1. **Aksamit, R. R., B. J. Howlett, and D. E. Koshland, Jr.** 1975. Soluble and membrane-bound aspartate-binding activities in *Salmonella typhimurium*. J. Bacteriol. **123**:1000–1005.
2. **Ames, G. F.** 1964. Uptake of amino acids by *Salmonella typhimurium*. Arch. Biochem. Biophys. **104**:1–18.
3. **Ammerman, J. W., and F. Azam.** 1982. Uptake of cyclic AMP by natural populations of marine bacteria. Appl. Environ. Microbiol. **43**:869–876.
4. **Anderson, J. J., and D. L. Oxender.** 1978. Genetic separation of high- and low-affinity transport systems for branched-chain amino acids in *Escherichia coli* K-12. J. Bacteriol. **136**:168–174.
5. **Anraku, Y.** 1978. Active transport of amino acids, p. 171–219. *In* B. P. Rosen (ed.), Bacterial transport. Marcel Dekker, Inc., New York.
6. **Anraku, Y., and L. A. Heppel.** 1967. On the nature of the changes induced in *Escherichia coli* by osmotic shock. J. Biol. Chem. **242**:2561–2569.
7. **Azam, F., and R. E. Hodson.** 1981. Multiphasic kinetics for D-glucose uptake by assemblages of natural marine bacteria. Mar. Ecol. Prog. Ser. **6**:213–222.
8. **Bai, B. M., C. V. Viswanathan, and S. C. Pillai.** 1962. Amino acids in sewage during treatment. J. Sci. Ind. Res. (India) **21**:72–76.
9. **Berger, E. A.** 1973. Different mechanisms of energy coupling for the active transport of proline and glutamine in *Escherichia coli*. Proc. Natl. Acad. Sci. U.S.A. **70**:1514–1518.
10. **Berger, E. A., and L. A. Heppel.** 1974. Different mechanisms of energy coupling for the shock-sensitive and shock-resistant amino acid permeases of *Escherichia coli*. J. Biol. Chem. **249**:7747–7755.
11. **Bright, J. J., and M. Fletcher.** 1983. Amino acid assimilation and respiration by attached and free-living populations of a marine *Pseudomonas* sp. Microb. Ecol. **9**:215–226.
12. **Clarke, S., and D. E. Koshland, Jr.** 1979. Membrane receptors for aspartate and serine in bacterial chemotaxis. J. Biol. Chem. **254**:9695–9702.
13. **Dills, S. S., A. Apperson, M. R. Schmidt, and M. H. Saier, Jr.** 1980. Carbohydrate transport in bacteria. Microbiol. Rev. **44**:385–418.
14. **Eighmy, T. T., D. Maratea, and P. L. Bishop.** 1983. Electron microscopic examination of wastewater biofilm formation and structural components. Appl. Environ. Microbiol. **45**:1921–1931.
15. **Engasser, J.-M., and C. Horvath.** 1976. Diffusion and kinetics with immobilized enzymes. Appl. Biochem. Bioeng. **1**:127–220.
16. **Fein, J. E., and R. A. MacLeod.** 1975. Characterization of neutral amino acid transport in a marine pseudomonad. J. Bacteriol. **124**:1177–1190.
17. **Gale, E. F., and J. M. Llewellin.** 1972. The role of hydrogen and potassium ions in the transport of acidic amino acids in *Staphylococcus aureus*. Biochim. Biophys. Acta **266**:182–205.
18. **Glover, G. I., S. M. D'Ambrosio, and R. A. Jensen.** 1975. Versatile properties of a nonsaturable, homogeneous transport system in *Bacillus subtilis*: genetic, kinetic, and affinity labeling studies. Proc. Natl. Acad. Sci. U.S.A. **72**:814–818.
19. **Griffiths, R. P., F. J. Hanus, and R. Y. Morita.** 1974. The effects of various water-sample treatments on the apparent uptake of glutamic acid by natural marine microbial populations. Can. J. Microbiol. **20**:1261–1266.
20. **Guardiola, J., M. De Felice, T. Klopotowski, and M. Iaccarino.** 1974. Multiplicity of isoleucine, leucine, and valine transport systems in *Escherichia coli* K-12. J. Bacteriol. **117**:382–392.
21. **Halpern, Y. S., and A. Even-Shoshan.** 1967. Properties of the glutamate transport system in *Escherichia coli*. J. Bacteriol. **93**:1009–1016.
22. **Halpern, Y. S., and M. Lupo.** 1965. Glutamate transport in wild-type and mutant strains of *Escherichia coli*. J. Bacteriol. **90**:1288–1295.
23. **Harold, F. M., and E. Spitz.** 1975. Accumulation of arsenate, phosphate, and aspartate by *Streptococcus faecalis*. J. Bacteriol. **122**:266–277.
24. **Horvath, C., and J.-M. Engasser.** 1974. External and internal diffusion in heterogeneous enzyme systems. Biotechnol. Bioeng. **16**:909–923.
25. **Hoshino, T.** 1979. Transport systems for branched-chain amino acids in *Pseudomonas aeruginosa*. J. Bacteriol. **139**:705–712.
26. **Joyce, G. H., and P. R. Dugan.** 1970. The role of floc-forming bacteria in BOD removal from waste water. Dev. Ind. Microbiol. **11**:337–386.
27. **Kahane, S., M. Marcus, E. Metzer, and Y. S. Halpern.** 1976. Glutamate transport in membrane vesicles of the wild-type strain and glutamate-utilizing mutants of *Escherichia coli*. J. Bacteriol. **125**:770–775.
28. **Kay, W. W.** 1971. Two aspartate transport systems in *Escherichia coli*. J. Biol. Chem. **246**:7373–7382.
29. **Kay, W. W.** 1978. Transport of carboxylic acids, p. 385–411. *In* B. P. Rosen (ed.), Bacterial transport. Marcel Dekker, Inc., New York.
30. **Kay, W. W., and M. J. Cameron.** 1978. Transport of C_4-

dicarboxylic acids in *Salmonella typhimurium*. Arch. Biochem. Biophys. **190**:281–289.
31. **Kiritani, K., and K. Ohnishi.** 1977. Repression and inhibition of transport systems for branched-chain amino acids in *Salmonella typhimurium*. J. Bacteriol. **129**:589–598.
32. **Klein, W. L., and P. D. Boyer.** 1972. Energization of active transport by *Escherichia coli*. J. Biol. Chem. **247**:7257–7265.
33. **Konings, W. N., A. Bisschop, and M. C. C. Daatselaar.** 1972. Transport of L-glutamate and L-aspartate by membrane vesicles of *Bacillus subtilis* W 23. FEBS Lett. **24**:260–264.
34. **Konings, W. N., and E. Freese.** 1972. Amino acid transport in membrane vesicles of *Bacillus subtilis*. J. Biol. Chem. **247**: 2408–2418.
35. **Kustu, S. G., N. C. McFarland, S. P. Hui, B. Esmon, and G. F.-L. Ames.** 1979. Nitrogen control in *Salmonella typhimurium*: co-regulation of synthesis of glutamine synthetase and amino acid transport systems. J. Bacteriol. **138**:218–234.
36. **La Motta, E. J.** 1976. External mass transfer in a biological film reactor. Biotechnol. Bioeng. **18**:1359–1370.
37. **La Motta, E. J.** 1976. Kinetics of growth and substrate uptake in a biological film system. Appl. Environ. Microbiol. **31**:286–293.
38. **Lombardi, F. J., and H. R. Kaback.** 1972. Mechanisms of active transport in isolated bacterial membrane vesicles. VIII. The transport of amino acids by membranes prepared from *Escherichia coli*. J. Biol. Chem. **247**:7844–7857.
39. **Miner, K. M., and L. Frank.** 1974. Sodium-stimulated glutamate transport in osmotically shocked cells and membrane vesicles of *Escherichia coli*. J. Bacteriol. **177**:1093–1098.
40. **Niven, D. F., and W. A. Hamilton.** 1974. Mechanisms of energy coupling to the transport of amino acids by *Staphylococcus aureus*. Eur. J. Biochem. **44**:517–522.
41. **Painter, H. A., and M. Viney.** 1959. Composition of a domestic sewage. J. Biochem. Microbiol. Tech. Eng. **1**:143–162.
42. **Painter, H. A., M. Viney, and A. Bywaters.** 1961. Composition of sewage and sewage effluents. Inst. Sewage Purif. J. Proc., p. 302–311.
43. **Rahmanian, M., D. R. Claus, and D. L. Oxender.** 1973. Multiplicity of leucine transport systems in *Escherichia coli* K-12. J. Bacteriol. **116**:1258–1266.
44. **Reid, K. G., N. M. Utech, and J. T. Holden.** 1970. Multiple transport components for dicarboxylic amino acids in *Streptococcus faecalis*. J. Biol. Chem. **245**:5261–5272.
45. **Ring, K., W. Gross, H. Ehle, and B. Foit.** 1977. Characterization of L-aspartate uptake by *Streptomyces hydrogenans*. J. Gen. Microbiol. **103**:307–317.
46. **Rorem, E. S.** 1955. Uptake of rubidium and phosphate ions by polysaccharide-producing bacteria. J. Bacteriol. **70**:691–701.
47. **Rosen, B. P., and E. R. Kashket.** 1978. Energetics of active transport, p. 559–620. *In* B. P. Rosen (ed.), Bacterial transport. Marcel Dekker, Inc., New York.
48. **Rosen, B. P., and F. D. Vasington.** 1971. Purification and characterization of a histidine binding protein from *Salmonella typhimurium* LT-2 and its relationship to the histidine permease system. J. Biol. Chem. **246**:5351–5360.
49. **Schellenberg, G. D., and C. E. Furlong.** 1977. Resolution of the multiplicity of the glutamate and aspartate transport systems of *Escherichia coli*. J. Biol. Chem. **252**:9055–9064.
50. **Short, S. A., D. C. White, and H. R. Kaback.** 1972. Mechanisms of active transport in isolated bacterial membrane vesicles. IX. The kinetics and specificities of amino acid transport in *Staphylococcus aureus* membrane vesicles. J. Biol. Chem. **247**: 7452–7458.
51. **Shuman, H. A.** 1982. Active transport of maltose in *Escherichia coli* K12. Role of the periplasmic maltose-binding protein and evidence for a substrate recognition site in the cytoplasmic membrane. J. Biol. Chem. **257**:5455–5461.
52. **Subrahmanyam, P. V. R., C. A. Sastry, A. V. S. P. Rao, and S. C. Pilla.** 1960. Amino acids in sewage sludges. J. Water Pollut. Control Fed. **32**:344–350.
53. **Vaccaro, R. F., and H. W. Jannasch.** 1966. Studies on the heterotrophic activity in seawater based on glucose assimilation. Limnol. Oceanogr. **11**:596–607.
54. **Whiteman, P. A., T. Iijima, M. D. Diesterhaft, and E. Freese.** 1978. Evidence for a low affinity but high velocity aspartate transport system needed for rapid growth of *Bacillus subtilis* on aspartate as sole carbon source. J. Gen. Microbiol. **107**:297–307.
55. **Willis, R. C., and C. E. Furlong.** 1975. Purification and properties of a periplasmic glutamate-aspartate binding protein from *Escherichia coli* K12 strain W3092. J. Biol. Chem. **250**: 2574–2580.
56. **Willis, R. C., and C. E. Furlong.** 1975. Interactions of a glutamate-aspartate binding protein with the glutamate transport system of *Escherichia coli*. J. Biol. Chem. **250**:2581–2586.
57. **Willis, R. C., and C. A. Woolfolk.** 1975. L-Asparagine uptake in *Escherichia coli*. J. Bacteriol. **123**:937–945.
58. **Wilson, D. B., and J. B. Smith.** 1978. Bacterial transport proteins, p. 495–557. *In* B. P. Rosen (ed.), Bacterial transport. Marcel Dekker, Inc., New York.
59. **Winne, D.** 1973. Unstirred layer, source of biased Michaelis constant in membrane transport. Biochim. Biophys. Acta **298**:27–31.
60. **Wood, J. M.** 1975. Leucine transport in *Escherichia coli*. The resolution of multiple transport systems and their coupling to metabolic energy. J. Biol. Chem. **250**:4477–4485.